Multi-Input Multi-Output Nonlinear Autopilot Design for Ship-to-Ship Missiles

Ki Hong Im, Dongkyoung Chwa, and Jin Young Choi*

Abstract: In this paper, a design method of nonlinear autopilot for ship-to-ship missiles is proposed. Ship-to-ship missiles have strongly coupled dynamics through roll, yaw, and pitch channel in comparison with general STT type missiles. Thus it becomes difficult to employ previous control design method directly since we should find three different solutions for each control fin deflection and should verify the stability for more complicated dynamics. In this study, we first propose a control loop structure for roll, yaw, and pitch autopilot which can determine the required angles of all three control fins. For yaw and pitch autopilot design, missile model is reduced to a minimum phase model by applying a singular perturbation like technique to the yaw and pitch dynamics. Based on this model, a multi-input multi-output (MIMO) nonlinear autopilot is designed. And the stability is analyzed considering roll influences on dynamic couplings of yaw and pitch channel as well as the aerodynamic couplings. Some additional issues on the autopilot implementation for these coupled missile dynamics are discussed. Lastly, 6-DOF (degree of freedom) numerical simulation results are presented to verify the proposed method.

Keywords: Nonlinear control, missiles, non-minimum phase, singular perturbation method, couplings, multi-input multi-output systems.

1. INTRODUCTION

Recently, there have been a lot of researches in the area of nonlinear autopilot design, which directly considered the nonlinearities in missile dynamics [1-9]. In particular, when the accelerations of the missile system are set to be controlled outputs, the input-output characteristics of the tail-controlled missile dynamics become non-minimum phase. Thus, well-known nonlinear control design methods such as the feedback linearization technique cannot be directly applied to the acceleration control of the tail-controlled missiles. To solve these problems, a method of partially linearizing control and singular perturbation like technique was proposed by approximating the non-minimum phase system into a minimum phase system [10-12].

In general, the nonlinear autopilot designs [10-12] were proposed for skid-to-turn (STT) missiles which have weak couplings between yaw and pitch dynamics while assuming the stabilization of the roll dynamics. However, the ship-to-ship missile considered in this paper has complicated couplings among roll, yaw, and pitch dynamics through wind angles (roll angle, angle-of-attack, and side slip angle) and three control fin deflections. Furthermore, the look-up tables for this ship-to-ship missile dynamics are given in terms of the total angle-of-attack and the bank angle instead of the angle-of-attack and the side-slip angle. Since these methods can no longer be directly employed, a control method needs to be developed for ship-to-ship missile with above aspects being considered.

This paper proposes an autopilot design consisting of the roll stabilizing controller and the yaw-pitch autopilot to achieve the satisfactory acceleration tracking performance. Firstly, overall control loop structure is proposed for the three channels to determine required control fin deflections easily. Since there are dominant aerodynamic coefficients for control inputs in each channel, the overall control loop for the ship-to-ship missile is divided into two parts; a roll dynamics stabilizer and a yaw-pitch autopilot. Secondly, a singular perturbation like technique is employed to the missile model so that it can be

Manuscript received February 28, 2005; revised October 6, 2005; accepted December 16, 2005. Recommended by past Editor-in-Chief Myung Jin Chung. This research was supported by the Engineering Research Institute at Seoul National University. The authors would like to thank the reviewers for their comments and suggestions.

Ki Hong Im and Jin Young Choi are with the School of Electrical Engineering and Computer Science, ASRI, Seoul National University, Gwanak P.O.Box 34(#048), Seoul 151-742, Korea (e-mails: khim@neuro.snu.ac.kr, jychoi@ee.snu.ac.kr).

Dongkyoung Chwa is with the Department of Electrical and Computer Engineering, Ajou University, San 5, Woncheon-Dong, Yeongtong-Gu, Suwon 443-749, Korea (e-mail: dkchwa @ajou.ac.kr).

* Corresponding author.

approximated to a minimum phase model. This minimum phase characteristics make it possible to design a feedback linearizing controller [11] and the yaw-pitch autopilot is designed by feedback linearization technique [13,14] in the MIMO structure. Through these steps, the proposed method achieves a decoupled acceleration tracking performance for both yaw and pitch channels but this makes the stability verification more complicated and difficult. Finally the overall stability is analyzed considering roll influences on dynamic couplings of yaw and pitch channel as well as the aerodynamic couplings. In addition, the paper discusses the issues of the implementation of the autopilots for coupled missile dynamics and, finally, presents the stability analysis of the overall missile control system.

The remainder of this paper is organized as follows. Firstly, an approximate minimum phase missile model is derived from the ship-to-ship missile dynamics. Then, the control loop is designed based on the minimum phase model and the stability is analyzed. Finally, the implementation issues are discussed, and the 6-DOF (degree of freedom) simulation results to verify the performance of the proposed autopilot are presented.

2. APPROXIMATE MINIMUM PHASE MODEL FOR SHIP-TO-SHIP MISSILES

In this section, ship-to-ship missile dynamics are presented together with their characteristics, and they are approximated to a minimum phase missile model by employing a partial feedback linearizing control input and singular perturbation like technique.

2.1. Ship-to-ship missile dynamics

The nonlinear missile dynamic equations with acceleration outputs are given by

$$\begin{cases} \dot{U} = rV - qW + \dfrac{T}{m} - \dfrac{QS}{m} C_x(\cdot) \\ \dot{p} = \dfrac{QSD}{I_M} C_l(\cdot) + \dfrac{HU}{I_M} C_{lp}\, p, \end{cases} \tag{1a}$$

$$\begin{cases} \dot{\beta} = -r + p\alpha + \dfrac{QS}{Um} C_y(\cdot) - \dfrac{QSDB}{Um} C_n(\cdot) - \dfrac{BH}{m} C_{nr} r \\ \dot{r} = \dfrac{QSD}{I_M} C_n(\cdot) - \dfrac{QSX_{cg}}{I_M} C_y(\cdot) + \dfrac{H}{I_M} U C_{nr} r \\ A_y = \dfrac{QS}{m} C_y(\cdot), \end{cases} \tag{1b}$$

$$\begin{cases} \dot{\alpha} = q - p\beta - \dfrac{QS}{Um} C_z(\cdot) + \dfrac{QSDB}{Um} C_m(\cdot) + \dfrac{BH}{m} C_{mq} q \\ \dot{q} = \dfrac{QSD}{I_M} C_m(\cdot) - \dfrac{QSX_{cg}}{I_M} C_z(\cdot) + \dfrac{H}{I_M} U C_{mq} q \\ A_z = -\dfrac{QS}{m} C_z(\cdot), \end{cases} \tag{1c}$$

where $H := 0.25\rho S\sqrt{D}$, $B := mX_{cg} / (I_M - mX_{cg}^2)$, $(\cdot) := (M_M, \alpha_T, \phi_A, \delta_E, \delta_O, \delta_R)$, and C_{lp}, C_{mq}, C_{nr} are dynamic derivatives. General assumptions were made to derive the missile model in (1), such as constant inertia and mass, yaw-pitch symmetry, and constant velocity. We introduce the following functions to simplify the design procedure.

$$C_a(M_M, \alpha_T, \phi_A) = C_{y0}(M_M, \alpha_T, \phi_A) + \frac{D}{l_f - l_g} C_{n0}(M_M, \alpha_T, \phi_A), \tag{2a}$$

$$C_b(M_M, \alpha_T, \phi_A) = C_{z0}(M_M, \alpha_T, \phi_A) + \frac{D}{l_f - l_g} C_{m0}(M_M, \alpha_T, \phi_A). \tag{2b}$$

Substituting (2a) and (2b) into (1b) and (1c), respectively, and using $h_v \equiv D/(l_f - l_g)$, yaw and pitch dynamic equations become

$$\begin{cases} \dot{\beta} = -r + p\alpha + \dfrac{QS(h_v + DB)}{Umh_v} C_y(\cdot) - \dfrac{QSDB}{Umh_v} C_a(\circ) - \dfrac{BH}{m} C_{nr} r \\ \dot{r} = -\dfrac{QS(X_{cg} h_v + D)}{I_M h_v} C_y(\cdot) + \dfrac{QSD}{I_M h_v} C_a(\circ) + \dfrac{H}{I_M} U C_{nr} r \\ A_y = \dfrac{QS}{m} C_y(\cdot), \end{cases} \tag{3a}$$

$$\begin{cases} \dot{\alpha} = q - p\beta - \dfrac{QS(h_v + DB)}{Umh_v} C_z(\cdot) - \dfrac{QSDB}{Umh_v} C_b(\circ) - \dfrac{BH}{m} C_{mq} q \\ \dot{q} = -\dfrac{QS(X_{cg} h_v + D)}{I_M h_v} C_z(\cdot) + \dfrac{QSD}{I_M h_v} C_b(\circ) + \dfrac{H}{I_M} U C_{mq} q \\ A_z = -\dfrac{QS}{m} C_z(\cdot), \end{cases} \tag{3b}$$

where $(\circ) := (M_M, \alpha_T, \phi_A)$, $(\cdot) := (\circ, \delta_E, \delta_O, \delta_R)$. However, since the coefficient functions, $C_{(\cdot)}(M_M, \alpha_T, \phi_A, \delta_E, \delta_O, \delta_R)$, $(\cdot) = x, y, z, \text{or } l$, have a form of (3) in our missile model, coefficient functions given in terms of α_T and ϕ_A are not suitable to be used with the control design method developed in terms of α and β. Therefore, we need to reformulate these aerodynamic coefficients into those parameterized by α and β such as $C_{(\cdot)\delta}(M_M, \alpha, \beta, \delta)$. These issues on implementation

problems will be discussed later. From here on, the coefficient functions will be denoted by $C_{(\cdot)\delta}$ for simplicity.

2.2. Approximate minimum phase model for ship-to-ship missile

Yaw and pitch control inputs are chosen as

$$\frac{u_y}{U} = -r + p\alpha + \frac{QS(h_v + DB)}{Umh_v} C_y - \frac{QSDB}{Umh_v} C_a - \frac{BH}{m} C_{nr} r, \tag{4a}$$

$$\frac{u_z}{U} = q - p\beta - \frac{QS(h_v + DB)}{Umh_v} C_z + \frac{QSDB}{Umh_v} C_b + \frac{BH}{m} C_{mq} q, \tag{4b}$$

where u_y and u_z are new control inputs for yaw and pitch dynamics, respectively, which will be determined later. Substituting (4a) and (4b) into (3a) and (3b), respectively, we obtain

$$\begin{cases} \dot{\beta} = \dfrac{u_y}{U} \\ \dot{r} = K_r r - \dfrac{QSD(BX_{cg} - 1)}{I_M (h_v + DB)} C_a - \dfrac{Um(X_{cg} h_v + D)}{I_M (h_v + DB)} \left\{ \dfrac{u_y}{U} - p\alpha \right\} \\ A_y = \left(\dfrac{(h_v + DB)}{Uh_v} \right)^{-1} \left\{ \dfrac{u_y}{U} - p\alpha + \dfrac{QSDB}{Umh_v} C_a + \left(1 + \dfrac{BH}{m} C_{nr} \right) r \right\}, \end{cases} \tag{5a}$$

$$\begin{cases} \dot{\alpha} = \dfrac{u_z}{U} \\ \dot{q} = K_q q - \dfrac{QSD(BX_{cg} - 1)}{I_M (h_v + DB)} C_b - \dfrac{Um(X_{cg} h_v + D)}{I_M (h_v + DB)} \left\{ -\dfrac{u_z}{U} - p\beta \right\} \\ A_z = -\left(\dfrac{(h_v + DB)}{Uh_v} \right)^{-1} \left\{ -\dfrac{u_z}{U} - p\beta + \dfrac{QSDB}{Umh_v} C_b + \left(1 + \dfrac{BH}{m} C_{mq} \right) q \right\}, \end{cases} \tag{5b}$$

where

$$K_r = -\frac{Um(X_{cg} h_v + D)}{I_M (h_v + DB)} \left(1 + \frac{BH}{m} C_{nr} \right) + \frac{H}{I_M} UC_{nr},$$

$$K_q = -\frac{Um(X_{cg} h_v + D)}{I_M (h_v + DB)} \left(1 + \frac{BH}{m} C_{mq} \right) + \frac{H}{I_M} UC_{mq}.$$

A direct application of feedback linearization technique to (5) can make the internal dynamics of this system unstable, since (5) is of non-minimum phase. This is a general characteristic of STT type missiles. Thus, we need to approximate the dynamics (5) to a minimum phase model.

The coefficients of r and q, K_r and K_q in (5), are physically very large values. Accordingly, r and q dynamics converge to their steady state values much faster than those of α and β. Here, we can assume that $\dot{r}$ and $\dot{q}$ are zero and accordingly, r and q can be reduced to their steady state value very quickly. That is, r dynamics can be replaced by its steady state values

$$r = -K_r^{-1} \left\{ -\frac{QSD(BX_{cg} - 1)}{I_M (h_v + DB)} C_a - \frac{Um(X_{cg} h_v + D)}{I_M (h_v + DB)} \left(\frac{u_y}{U} - p\alpha \right) \right\}. \tag{6}$$

Thus, (5a) and (5b) can be reduced as

$$\begin{cases} \dot{\bar{\beta}} = \dfrac{\bar{u}_y}{U} \\ \bar{A}_y = \dfrac{QSD}{(X_{cg} h_v + D)m} \bar{C}_a + \dfrac{Hh_v}{(X_{cg} h_v + D)m} UC_{nr} \bar{r}, \end{cases} \tag{7a}$$

$$\begin{cases} \dot{\bar{\alpha}} = \dfrac{\bar{u}_z}{U} \\ \bar{A}_z = -\dfrac{QSD}{(X_{cg} h_v + D)m} \bar{C}_b - \dfrac{Hh_v}{(X_{cg} h_v + D)m} UC_{mq} \bar{q}, \end{cases} \tag{7b}$$

where the over bars are used to distinguish the variables of reduced system from those of original dynamics. The dynamics in (7) are minimum phase since the internal dynamics are stable. The error dynamics between the original dynamics and the reduced minimum phase dynamics will be considered in the following section through the stability analysis.

3. CONTROL LOOP DESIGN AND STABILITY ANALYSIS

In this section, we design control loops for ship-to-ship missiles and analyze the stabilities. First, to simplify the structure of controller for roll, yaw, and pitch channels, we design the missile velocity control loop. If we design the thrust force in (1a) as

$$T = -m \left\{ rV - qW - \frac{QS}{m} C_x + k_u (U - U_d) \right\}, \tag{8}$$

where U_d is a reference velocity input and k_u is a positive design parameter, then the velocity dynamics in (1a) with thrust in (8) become the stable dynamics as follows.

$$\dot{U} = -k_u U + k_u U_d \tag{9}$$

Remark 1: The velocity U can be almost fixed as the constant U_d by the velocity controller (8) and, thus, Mach number could be assumed to be fixed in the sense that $U \cong M_M$.

The following should be considered further in the design of other control loops. The missile model in this paper has relatively strong couplings not only in the aerodynamic coefficients through control fin deflections, but also in yaw and pitch dynamics through state variables. However, the couplings between roll dynamics and yaw-pitch dynamics can be weakened if p remains sufficiently small. The design of the roll stabilizer is possible only when the roll dynamics is independent of other dynamics. However, aerodynamic functions have additional couplings through control fin deflections since they include the control fin deflections of other channels and given as $C_{(\cdot)}(\cdots, \delta_E, \delta_O, \delta_R)$, $(\cdot) = x, y, z, \text{or } l$. Accordingly, it becomes difficult to solve each of the control fin deflections directly. To solve these problems, we propose the overall control loop structure as shown in Fig. 1. This figure represents the control structure with two main control blocks, interconnected by feedback loop. One of the blocks is the controller of the roll dynamics determining control fin command, δ_R^c, and the other is the controller of the yaw-pitch dynamics determining δ_E^c and δ_O^c. The roll aerodynamic coefficient function is given by

$$\begin{aligned} C_l = {} & C_{l0}(M, \alpha, \beta) + C_{l\delta_E}(\cdots, \delta_E) \\ & + C_{l\delta_O}(\cdots, \delta_O) + C_{l\delta_R}(\cdots, \delta_R), \end{aligned} \tag{10}$$

where $C_{l\delta R}$ and $C_{l\delta E} + C_{l\delta O}$ are controllable parts, and $C_{l\delta R}$ is relatively larger than $C_{l\delta E} + C_{l\delta O}$. Therefore, we can assume that $C_{l\delta R}$ is a dominant term in roll dynamics control, whereas $C_{y\delta O}$ and $C_{y\delta E}$ are dominant terms for yaw-pitch dynamics. In Fig. 1, the aerodynamic coupling through control inputs are considered by the feedback structure of the proposed controller such that the dominant aerodynamic coefficients can be designed well enough to eliminate the effects from the other coefficients. Since yaw and pitch dynamics have strong couplings through control fin deflections δ_E, δ_O and wind angles, we will proceed with the autopilot design for yaw-pitch channel in MIMO form. The characteristics of the yaw-pitch aerodynamic coefficients will be explained in more detail in the next subsection.

First, in order to make the roll dynamics stable, we make $C_{l\delta R}$ equal to the control input

$$u_p = C_{l\delta R} \tag{11}$$

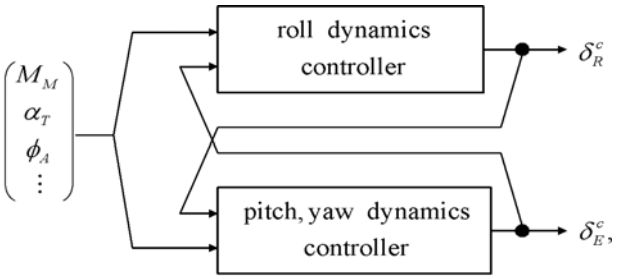

Fig. 1. Structure of overall control loop.

by designing this input as

$$\begin{aligned} u_p = {} & \left(\frac{QSD}{I_M}\right)^{-1} \left\{ v_p - \frac{HU}{I_M} C_{lp}\, p \right\} \\ & - C_{l0} - C_{l\delta E} - C_{l\delta O}, \end{aligned} \tag{12}$$

where v_p is a compensator variable, and fin commands δ_E^c and δ_O^c can be determined from yaw-pitch autopilot in Fig. 1. If we design the compensator as

$$v_p = -k_p p - k_\phi \phi,$$

where $\dot{\phi} \cong p$ is a roll angular rate and k_p, k_ϕ are positive design parameters, the roll dynamics become

$$\ddot{\phi} = -k_p \dot{\phi} - k_\phi \phi, \tag{13}$$

which verifies that ϕ and p remain bounded and converge to zero.

For designing the control loops, the following assumptions are made.

Assumption 1: The variations of C_{lp}, C_{mq}, and C_{nr} are negligible ($\dot{C}_{lp} = \dot{C}_{mq} = \dot{C}_{nr} = 0$).

Assumption 2: The controlled roll dynamics can work independently of yaw-pitch dynamics.

Remark 2: In general, dynamic derivatives in Assumption 1 can be included in nonlinear missile modeling in order to bring the missile model closer to the actual missile system. However, we can assume that those parameters remain constant since these parameters are slowing varying enough to be considered as fixed values.

Remark 3: Assumption 2 is similar to or weaker than assumptions that are usually made such that roll angle is zero or the roll rate is zero, i.e., $\phi = 0$, $p = 0$ [15]. The roll dynamics has inherently weak couplings with yaw-pitch dynamics, and also those small coupling terms are eliminated by the designed roll control loop.

Before discussing the yaw-pitch control design and its stability analysis, we characterize the properties of yaw-pitch aerodynamic coefficients. For this, the following assumption is made.

Assumption 3: $C_a(\alpha, \beta)$ and $C_b(\alpha, \beta)$ in (2)

satisfy the conditions as follows:

i) C_a and C_b are smooth functions with respect to α and β.

ii) C_a and C_b are strictly increasing in β and α, respectively.

iii) The partial derivatives satisfy

$$\left|\frac{\partial C_a}{\partial \alpha}\right| < \left|\frac{\partial C_a}{\partial \beta}\right|, \quad \left|\frac{\partial C_b}{\partial \beta}\right| < \left|\frac{\partial C_b}{\partial \alpha}\right|. \tag{14}$$

iv) The inverse of the partial derivatives, $\left(\frac{\partial C_a}{\partial \beta}\right)^{-1}$ and $\left(\frac{\partial C_b}{\partial \alpha}\right)^{-1}$, are bounded.

Remark 4: The first and second conditions in Assumption 3 characterize the properties of the general shape of aerodynamic coefficient functions. The third condition states that, in our missile system, the coefficient function C_a has dominant variation in β whereas C_b does in α even though those coefficients are strongly coupled and can be varied with α and β simultaneously. If the third condition is not satisfied, the dominant aerodynamics could changes conversely, which is not realistic for conventional STT missiles in that the autopilot can not be constructed properly. The fourth condition follows from the second condition and will be considered in the stability analysis.

The approximate minimum phase missile model derived in Section 2 is expressed here again for convenience.

$$\begin{cases} \dot{\bar{\beta}} = \dfrac{\bar{u}_y}{U} \\ \bar{r} = -K_r^{-1}\left\{-\dfrac{QSD(BX_{cg}-1)}{I_M(h_v+DB)}\bar{C}_a \right. \\ \qquad \left. -\dfrac{Um(X_{cg}h_v+D)}{I_M(h_v+DB)}\left(\dfrac{\bar{u}_y}{U}-p\bar{\alpha}\right)\right\} \\ \bar{A}_y = \dfrac{QSD}{(X_{cg}h_v+D)m}\bar{C}_a + \dfrac{Hh_v}{(X_{cg}h_v+D)m}UC_{nr}\bar{r}, \end{cases} \tag{15a}$$

$$\begin{cases} \dot{\bar{\alpha}} = \dfrac{\bar{u}_z}{U} \\ \bar{q} = -K_q^{-1}\left\{-\dfrac{QSD(BX_{cg}-1)}{I_M(h_v+DB)}\bar{C}_b \right. \\ \qquad \left. -\dfrac{Um(X_{cg}h_v+D)}{I_M(h_v+DB)}\left(-\dfrac{\bar{u}_z}{U}-p\bar{\beta}\right)\right\} \\ \bar{A}_z = -\dfrac{QSD}{(X_{cg}h_v+D)m}\bar{C}_b - \dfrac{Hh_v}{(X_{cg}h_v+D)m}UC_{mq}\bar{q}. \end{cases} \tag{15b}$$

Here, we define the Jacobian matrices of the coefficient functions as

$$A_{uv} \equiv \begin{bmatrix} \dfrac{\partial C_a}{\partial \beta} & \dfrac{\partial C_a}{\partial \alpha} \\ -\dfrac{\partial C_b}{\partial \beta} & -\dfrac{\partial C_b}{\partial \alpha} \end{bmatrix}, \quad \bar{A}_{uv} \equiv \begin{bmatrix} \dfrac{\partial \bar{C}_a}{\partial \bar{\beta}} & \dfrac{\partial \bar{C}_a}{\partial \bar{\alpha}} \\ -\dfrac{\partial \bar{C}_b}{\partial \bar{\beta}} & -\dfrac{\partial \bar{C}_b}{\partial \bar{\alpha}} \end{bmatrix}. \tag{16}$$

Nonlinear autopilot design for yaw-pitch dynamics can be summarized as follows.

Proposition 1 (Autopilot Design for Ship-to-Ship Missile)**:** If we design control inputs for (15a) and (15b) as

$$\begin{aligned} \bar{C}_y = &\left(\frac{QS(h_v+DB)}{Umh_v}\right)^{-1}\left\{\frac{\bar{u}_y}{U} - p\bar{\alpha}\right. \\ &\left. + \frac{QSDB}{Umh_v}\bar{C}_a + \left(1+\frac{BH}{m}C_{nr}\right)\bar{r}\right\}, \end{aligned} \tag{17a}$$

$$\begin{aligned} \bar{C}_z = &\left(\frac{QS(h_v+DB)}{Umh_v}\right)^{-1}\left\{-\frac{\bar{u}_z}{U} - p\bar{\beta}\right. \\ &\left. + \frac{QSDB}{Umh_v}\bar{C}_b + \left(1+\frac{BH}{m}C_{mq}\right)\bar{q}\right\}, \end{aligned} \tag{17b}$$

where the control inputs are chosen as

$$\begin{pmatrix} \bar{u}_y \\ \bar{u}_z \end{pmatrix} = \left(\frac{QSD}{(X_{cg}h_v+D)Um}\right)^{-1} \cdot \bar{A}_{uv}^{-1}\begin{pmatrix} \bar{v}_y \\ \bar{v}_z \end{pmatrix} \tag{18}$$

and the compensator is designed as

$$\begin{cases} \dot{\bar{v}}_y = -\theta_1\bar{v}_y + \theta_2(A_{yc} - \bar{A}_y) \\ \dot{\bar{v}}_z = -\theta_1\bar{v}_z + \theta_2(A_{zc} - \bar{A}_z), \end{cases} \tag{19}$$

then the acceleration outputs of the missile system in (15) follows that of the linear reference model $\ddot{\bar{A}}_{y(z)} + \theta_1\dot{\bar{A}}_{y(z)} + \theta_2\bar{A}_{y(z)} = \theta_2 A_{yc(zc)}$, where θ_1 and θ_2 are positive design parameters.

Proof: Using Assumption 1 and differentiating the outputs of (15a) and (15b), $\bar{A}_y$ and $\bar{A}_z$, with respect to time, we have

$$\begin{aligned} \dot{\bar{A}}_y &= \frac{QSD}{(X_{cg}h_v+D)m}\dot{\bar{C}}_a + \frac{Hh_v}{(X_{cg}h_v+D)m}UC_{nr}\dot{\bar{r}} \\ &= \frac{QSD}{(X_{cg}h_v+D)Um}\left\{\frac{\partial \bar{C}_a}{\partial \bar{\alpha}}\bar{u}_z + \frac{\partial \bar{C}_a}{\partial \bar{\beta}}\bar{u}_y\right\} \\ &\quad + \frac{Hh_v}{(X_{cg}h_v+D)m}UC_{nr}\dot{\bar{r}} \end{aligned}$$

$$\dot{\bar{A}}_z = -\frac{QSD}{(X_{cg}h_v+D)m}\dot{\bar{C}}_b - \frac{Hh_v}{(X_{cg}h_v+D)m}UC_{mq}\dot{\bar{q}}$$

$$= \frac{QSD}{(X_{cg}h_v + D)Um}\left\{-\frac{\partial \bar{C}_b}{\partial \bar{\alpha}}\bar{u}_z - \frac{\partial \bar{C}_b}{\partial \bar{\beta}}\bar{u}_y\right\} - \frac{Hh_v}{(X_{cg}h_v + D)m}UC_{mq}\dot{\bar{q}} \quad .$$

Also, since $\dot{\bar{r}}$ and $\dot{\bar{q}}$ are zeros in this model, above equations yield

$$\begin{pmatrix}\dot{\bar{A}}_y \\ \dot{\bar{A}}_z\end{pmatrix} = \left(\frac{QSD}{(X_{cg}h_v + D)Um}\right)\cdot \bar{A}_{uv}\cdot\begin{pmatrix}\bar{u}_y \\ \bar{u}_z\end{pmatrix} = \begin{pmatrix}\bar{v}_y \\ \bar{v}_z\end{pmatrix}. \quad (20)$$

Consequently, we have

$$\begin{aligned}\ddot{\bar{A}}_y &= -\theta_1\bar{v}_y + \theta_2(A_{yc} - \bar{A}_y) \\ &= -\theta_1\dot{\bar{A}}_y + \theta_2(A_{yc} - \bar{A}_y),\end{aligned} \quad (21a)$$

$$\begin{aligned}\ddot{\bar{A}}_z &= -\theta_1\bar{v}_z + \theta_2(A_{zc} - \bar{A}_z) \\ &= -\theta_1\dot{\bar{A}}_z + \theta_2(A_{zc} - \bar{A}_z).\end{aligned} \quad (21b)$$

□

Here, we can find that the coupled yaw and pitch channels are now decoupled as in (21) and behave as second-order reference models when there is no error in the approximate minimum phase model.

Since control input and compensators in (18) and (19) should be replaced by actual values as

$$\begin{pmatrix}u_y \\ u_z\end{pmatrix} = \left(\frac{QSD}{(X_{cg}h_v + D)Um}\right)^{-1}\cdot A_{uv}^{-1}\begin{pmatrix}v_y \\ v_z\end{pmatrix}, \quad (22)$$

$$\begin{cases}\dot{v}_y = -\theta_1 v_y + \theta_2(A_{yc} - A_y) \\ \dot{v}_z = -\theta_1 v_z + \theta_2(A_{zc} - A_z),\end{cases} \quad (23)$$

we need to describe the error dynamics between (5) and (15) in order to analyze the stability and performance for MIMO autopilot for yaw-pitch channels.

Proposition 2 (Error Dynamics)**:** The error dynamics between (5) and (15) is given as

$$\begin{cases}\dot{e}_v = -\theta_1 e_v - \theta_2 e_\eta - \theta_2 A_1 e_0 \\ \dot{e}_\eta = e_v \\ \dot{e}_0 = A_2 e_0 + \dot{h} \\ e_A = A_1 e_0 + e_\eta,\end{cases} \quad (24)$$

where

$$e_v = \begin{pmatrix}e_{vy} \\ e_{vz}\end{pmatrix} = \begin{pmatrix}v_y - \bar{v}_y \\ v_z - \bar{v}_z\end{pmatrix}, \quad (25a)$$

$$e_\eta = \begin{pmatrix}e_{\eta a} \\ e_{\eta b}\end{pmatrix} = \frac{QSD}{(X_{cg}h_v + D)m}\cdot\begin{pmatrix}C_a - \bar{C}_a \\ -C_b + \bar{C}_b\end{pmatrix}, \quad (25b)$$

$$e_0 = \begin{pmatrix}e_{r0} \\ e_{q0}\end{pmatrix} = \begin{pmatrix}r_0 - \bar{r}_0 \\ q_0 - \bar{q}_0\end{pmatrix}, e_A = \begin{pmatrix}e_{Ay} \\ e_{Az}\end{pmatrix} = \begin{pmatrix}A_y - \bar{A}_y \\ A_z - \bar{A}_z\end{pmatrix}, \quad (26)$$

and

$$A_1 = \begin{bmatrix}\frac{h_v(HUC_{nr} - K_r I)}{m(X_{cg}h_v + D)} & 0 \\ 0 & \frac{h_v(HUC_{mq} + K_q I)}{m(X_{cg}h_v + D)}\end{bmatrix}, \quad (27a)$$

$$A_2 = \begin{bmatrix}K_r & 0 \\ 0 & K_q\end{bmatrix}, \quad (27b)$$

$$h = \begin{pmatrix}h_y \\ h_z\end{pmatrix} = \frac{1}{I(h_v + DB)}\begin{pmatrix}K_r^{-1}\{-QSD(BX_{cg} - 1)C_a - Um(X_{cg}h_v + D)(u_y/U - p\alpha)\} \\ K_q^{-1}\{-QSD(BX_{cg} - 1)C_b - Um(X_{cg}h_v + D)(-u_z/U - p\beta)\}\end{pmatrix}, \quad (28)$$

$$\begin{pmatrix}r_0 \\ q_0\end{pmatrix} = \begin{pmatrix}r \\ q\end{pmatrix} + h, \quad (29)$$

whereas

$$\bar{h} = \begin{pmatrix}\bar{h}_y \\ \bar{h}_z\end{pmatrix} = \frac{1}{I(h_v + DB)}\begin{pmatrix}K_r^{-1}\{-QSD(BX_{cg} - 1)\bar{C}_a - Um(X_{cg}h_v + D)(u_y/U - p\bar{\alpha})\} \\ K_q^{-1}\{-QSD(BX_{cg} - 1)\bar{C}_b - Um(X_{cg}h_v + D)(-u_z/U - p\bar{\beta})\}\end{pmatrix}, \quad (30)$$

$$\begin{pmatrix}\bar{r}_0 \\ \bar{q}_0\end{pmatrix} = \begin{pmatrix}\bar{r} \\ \bar{q}\end{pmatrix} + \bar{h}. \quad (31)$$

Proof: Together with (22) and (23), the coupled yaw-pitch dynamics in (5) give the closed loop system as follows.

$$\begin{pmatrix}\dot{\alpha} \\ \dot{\beta}\end{pmatrix} = \left(\frac{QSD}{(X_{cg}h_v + D)m}\right)^{-1}\cdot A_{uv}^{-1}\cdot\begin{pmatrix}v_y \\ v_z\end{pmatrix}, \quad (32a)$$

$$\begin{cases}\dot{v}_y = -\theta_1 v_y + \theta_2(A_{yc} - A_y) \\ \dot{v}_z = -\theta_1 v_z + \theta_2(A_{zc} - A_z),\end{cases} \quad (32b)$$

$$\begin{cases}\dot{r} = K_r r - \frac{QSD(BX_{cg} - 1)}{I_M(h_v + DB)}C_a - \frac{Um(X_{cg}h_v + D)}{I_M(h_v + DB)}(\frac{u_y}{U} - p\alpha) \\ \dot{q} = K_q q - \frac{QSD(BX_{cg} - 1)}{I_M(h_v + DB)}C_b - \frac{Um(X_{cg}h_v + D)}{I_M(h_v + DB)}(-\frac{u_z}{U} - p\beta),\end{cases} \quad (32c)$$

$$\begin{cases} A_y = \left(\dfrac{(h_v + DB)}{Uh_v}\right)^{-1} \left\{ \dfrac{u_y}{U} - p\alpha + \dfrac{QSDB}{Umh_v} C_a + (1 + \dfrac{BH}{m} C_{nr}) r \right\} \\ A_z = -\left(\dfrac{(h_v + DB)}{Uh_v}\right)^{-1} \left\{ -\dfrac{u_z}{U} - p\beta + \dfrac{QSDB}{Umh_v} C_b + (1 + \dfrac{BH}{m} C_{mq}) q \right\}. \end{cases} \quad (32d)$$

Introducing the notations in (29), (32c) and (32d), this system can be reformulated as

$$\begin{cases} \dot{r}_0 = K_r r_0 + \dot{h}_y \\ \dot{q}_0 = K_q q_0 + \dot{h}_z, \end{cases} \quad (33a)$$

$$\begin{cases} A_y = \left(-K_r \dfrac{Ih_v}{m(Xh_v + D)} \right) r_0 \\ \qquad + \dfrac{QSD}{m(X_{cg} h_v + D)} C_a + \dfrac{HUh_v C_{nr}}{m(X_{cg} h_v + D)} r_0 \\ A_z = \left(K_q \dfrac{Ih_v}{m(Xh_v + D)} \right) q_0 \\ \qquad - \dfrac{QSD}{m(X_{cg} h_v + D)} C_b - \dfrac{HUh_v C_{mq}}{m(X_{cg} h_v + D)} q_0. \end{cases} \quad (33b)$$

Also, the reduced system in (15) can be expressed as follows: Together with

$$\begin{pmatrix} \bar{r}_0 \\ \bar{q}_0 \end{pmatrix} = \begin{pmatrix} \bar{r} \\ \bar{q} \end{pmatrix} + \bar{h} = \begin{pmatrix} 0 \\ 0 \end{pmatrix}, \quad (34)$$

the reduced system in (15) and (19) become

$$\begin{pmatrix} \dot{\bar{\alpha}} \\ \dot{\bar{\beta}} \end{pmatrix} = \left(\frac{QSD}{(X_{cg} h_v + D)m} \right)^{-1} \cdot \bar{A}_{uv}^{-1} \cdot \begin{pmatrix} \bar{v}_y \\ \bar{v}_z \end{pmatrix}, \quad (35a)$$

$$\begin{cases} \dot{\bar{v}}_y = -\theta_1 \bar{v}_y + \theta_2 (A_{yc} - \bar{A}_y) \\ \dot{\bar{v}}_z = -\theta_1 \bar{v}_z + \theta_2 (A_{zc} - \bar{A}_z), \end{cases} \quad (35b)$$

$$\begin{cases} \dot{\bar{r}}_0 = 0 \\ \dot{\bar{q}}_0 = 0, \end{cases} \quad (35c)$$

$$\begin{cases} \bar{A}_y = \dfrac{QSD}{m(X_{cg} h_v + D)} \bar{C}_a + \dfrac{HUh_v C_{nr}}{m(X_{cg} h_v + D)} \bar{r} \\ \bar{A}_z = -\dfrac{QSD}{m(X_{cg} h_v + D)} \bar{C}_b - \dfrac{HUh_v C_{mq}}{m(X_{cg} h_v + D)} \bar{q}. \end{cases} \quad (35d)$$

Taking the time derivative of e_η in (25), we have

$$\dot{e}_\eta = \begin{pmatrix} \dot{e}_{\eta a} \\ \dot{e}_{\eta b} \end{pmatrix} = \frac{QSD}{(X_{cg} h_v + D)m} \left\{ A_{uv} \begin{pmatrix} \dot{\beta} \\ \dot{\alpha} \end{pmatrix} - \bar{A}_{uv} \begin{pmatrix} \dot{\bar{\beta}} \\ \dot{\bar{\alpha}} \end{pmatrix} \right\} = e_v \quad (36)$$

and the output error e_A in (24) can be obtained as

$$e_A = \begin{pmatrix} -K_r \dfrac{Ih_v}{m(Xh_v + D)} r_0 + \dfrac{HUh_v C_{nr}}{m(X_{cg} h_v + D)} (r - \bar{r}) \\ + \dfrac{QSD}{m(X_{cg} h_v + D)} (C_a - \bar{C}_a) \\ K_q \dfrac{Ih_v}{m(Xh_v + D)} q_0 - \dfrac{HUh_v C_{mq}}{m(X_{cg} h_v + D)} (q - \bar{q}) \\ - \dfrac{QSD}{m(X_{cg} h_v + D)} (C_b - \bar{C}_b) \end{pmatrix} \quad (37)$$
$$= A_1 e_0 + e_\eta.$$

The third row of (24) is obtained from (33a), and the first row of (24) is obtained from (32b), (35b), and (37). □

The following theorem shows the stability and performance analysis for the coupled yaw and pitch error dynamics and use Propositions 1 and 2 when considering the error dynamics in (24) generated by singular perturbation like technique.

Theorem 1 (Stability Analysis of Error Dynamics)**:** The error dynamics in (24) is stable in the sense that the tracking error $e_{YZ} = (A_{yc} - A_y \;\; A_{zc} - A_z)^T$ is uniformly ultimately bounded.

Proof : See Appendix A.

Remark 5: Note that the tracking error in (A6b) is bounded and depends on the combinations of $H_i^*, i = 1,2,3$, which in turn depends on initial condition and $\|A_2^{-1}\|$. Since $\|A_2^{-1}\|$ is a sufficiently small value, we can expect that $e_0(t)$ will remain in a small neighborhood of zero after sufficient time. Accordingly, the ultimate bound of the tracking error in Theorem 1 can be said to also be dependent on $\|A_2^{-1}\|$, and can be smaller when $\|A_2^{-1}\|$ becomes small. Thus, when $\|A_2^{-1}\|$ decreases to zero, it is possible to recover the asymptotic stability.

4. IMPLEMENTATION ISSUES

In the case where the control loops have a form as discussed in Section 3 and the missiles have strong couplings as in the case of the ship-to-ship missiles considered herein, some additional issues considering the implementation of this autopilot needs to be discussed as follows. Since the coefficient functions, $C_{(\cdot)}(M_M, \cdots)$, $(\cdot) = x, y, z,$ or l, have a form of (3), the coefficient functions in α_T and ϕ_A in Section 3 shall not be suitable to apply the control design method for coefficient functions in α and β and will have to overcome the following obstacle.

Fig. 2 shows the states in the $Y - Z$ plane of body axis when acceleration commands are given such that the velocity vector passes through the origin. It should

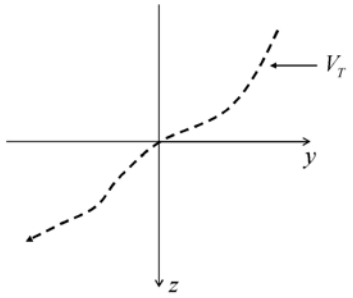

(a) Trajectory of the missile velocity.

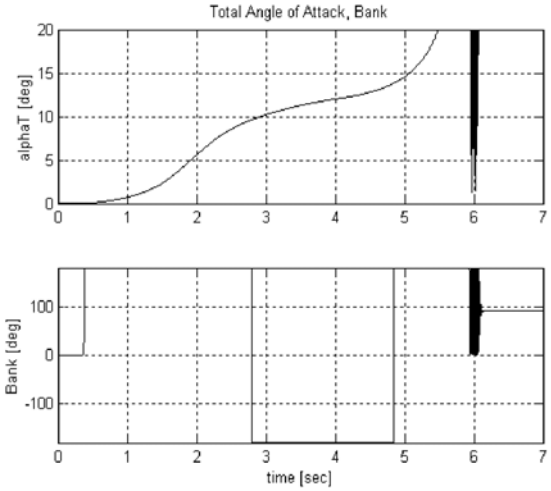

(b) Variations of α_T and ϕ_A

Fig. 2. History of states with missile maneuver.

be noted that the instant jump phenomenon of bank angle ϕ_A occurs with these acceleration commands. This can be clearly verified through the following equation, where $\dot{\phi}_A$ becomes unbounded as α and β approach to zero.

$$\dot{\alpha}_T \cong \cos^2(\alpha_T)\left\{\frac{\alpha}{\sqrt{\alpha^2+\beta^2}}\dot{\alpha}+\frac{\beta}{\sqrt{\alpha^2+\beta^2}}\dot{\beta}\right\}$$
$$= \cos^2(\alpha_T)\{\cos(\phi_A)\dot{\alpha}+\sin(\phi_A)\dot{\beta}\},$$
$$\dot{\phi}_A \cong \cos^2(\phi_A)\left\{\frac{\alpha\dot{\beta}-\dot{\alpha}}{\alpha^2}\right\}=\frac{\alpha\dot{\beta}-\dot{\alpha}}{\alpha^2+\beta^2}$$
$$= \frac{1}{\sqrt{\alpha^2+\beta^2}}\{-\sin(\phi_A)\dot{\alpha}+\cos(\phi_A)\dot{\beta}\}$$

Accordingly, the parametric model of α_T and ϕ_A is not appropriate to be applied to the nonlinear control design schemes such as feedback linearization because these methods require the differentiation of the aerodynamic coefficients given as follows:

$$\frac{d}{dt}C_{(\cdot)}(\alpha_T,\phi_A)=\frac{\partial C}{\partial \alpha_T}\dot{\alpha}_T+\frac{\partial C}{\partial \phi_A}\dot{\phi}_A.$$

Considering the above, coefficient functions in α and β is organized by reformulating the existing coefficient functions of α_T and ϕ_A, and the relations between these variables are given by

$$\begin{cases}\tan\alpha_T=\sqrt{\tan^2\alpha+\tan^2\beta}\\ \tan\phi_A=\dfrac{\tan\alpha}{\tan\beta}.\end{cases} \tag{38}$$

That is, by using (38) and taking coordinate transformations for $C_{(\cdot)\delta_{(\circ)}}(M_M,\alpha_T,\phi_A,\delta_{(\circ)})$ and $C_{(\cdot)}(M_M,\alpha_T,\phi_A)$, $(\cdot)=x_0,y_0,z_0,l_0,a,$ or b, where $(\cdot)=x,y,z,$ or l, $(\circ)=E,O,$ or R, we can have the reformulated coefficient functions

$$C^{\alpha\beta}_{(\cdot)\delta_{(\circ)}}(M_M,\alpha,\beta,\delta_{(\circ)})$$
$$\equiv C_{(\cdot)\delta_{(\circ)}}\left(M_M,\tan^{-1}\{\sqrt{\tan^2\alpha+\tan^2\beta}\},\frac{\tan\alpha}{\tan\beta},\delta_{(\circ)}\right),$$
$$C^{\alpha\beta}_{(\cdot)}(M_M,\alpha,\beta)$$
$$\equiv C_{(\cdot)}\left(M_M,\tan^{-1}\{\sqrt{\tan^2\alpha+\tan^2\beta}\},\frac{\tan\alpha}{\tan\beta}\right),$$

where $(\cdot)=x_0,y_0,z_0,l_0,a,$ or b.

Fig. 3 describes this relation. Note that the reformulated coefficient functions given by (38) have the same values as the original ones.

Another issue that must be dealt with is the calculation of the actual control fin deflections. Since the ship-to-ship missile uses non-affine, coupled aerodynamic coefficients through control fin deflections, it is not easy to determine the control fin

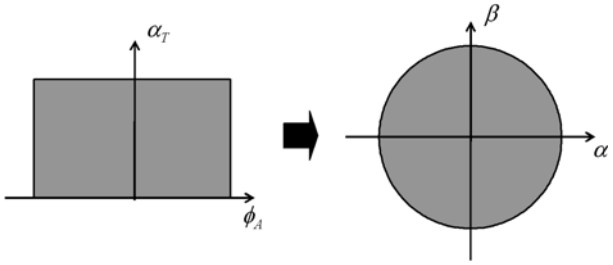

Fig. 3. Reformulation of aerodynamic coefficients through coordinate transformation.

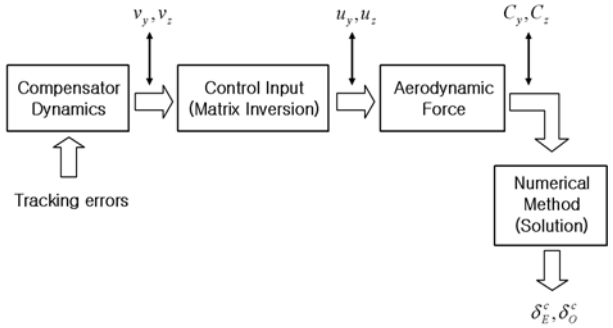

Fig. 4. Calculation of control fin deflections.

deflections analytically. Thus, after calculating the desired value of aerodynamic coefficient as given in (17), control fin deflections need to be calculated by employing numerical methods. The overall procedure for obtaining control fin deflections is illustrated in Fig. 4.

5. NUMERICAL SIMULATIONS

In this section, the overall control loops designed in Section 3 are applied to 6-DOF ship-to-ship missile model for simulations. Although we assumed constant inertia and mass, yaw-pitch symmetry, and constant velocity in designing the autopilot, we considered them as time-varying variables in the simulations. Also, all of the designed control loops such as velocity control loop, roll stabilization loop, and yaw-pitch autopilot loop are included.

Design parameters are set as follows: $U_d = 238m/s$, $k_u = 100$ for the velocity control loop; $k_p = 5$, $k_\phi = 10$ for the roll stabilization loop; and $\theta_1 = 2 \times 0.707$, $\theta_2 = 1$ for yaw-pitch autopilot loop. Actuator model for control fin operation is set to be a first-order low pass filter with the form $\tau\dot{\delta}_{(\cdot)} = -\delta_{(\cdot)} + \delta^c_{(\cdot)}$, $(\cdot) = E, O, R$ for the time constant $\tau = 10ms$.

Figs. 5 and 6 present the simulation results when the acceleration commands are given as square wave functions with maximum values of $\pm 2g$ and $\pm 3g$, respectively. As can be seen from these figures, all of the states and control inputs, with the exception of the thrust force, appear to be unsaturated and the overall control loop operates properly. The tracking results in Figs. 5(a) and 6(a) show the decoupled response between yaw and pitch accelerations. Since the strong coupling between yaw and pitch dynamics are effectively compensated by the feedback linearization in MIMO structure. Figs. 5(b) and 6(b) show the velocities using the thrust force in Figs. 5(g) and 6(g), respectively. We can see that thrust force is relatively independent of other dynamics and is insensitive to the saturation effect. Figs 5(c), 5(d), 6(c), and 6(d) show the result of roll angle and roll rate control. In both cases, roll dynamics is seen to be well stabilized and the roll angle to remain sufficiently small even when the perturbation range becomes wider with larger acceleration commands.

Lastly, we can observe that the couplings between roll control fin deflections and yaw-pitch control fin deflections are compensated properly by applying the proposed overall control loop structure. Even though the bank angle ϕ_A changes discontinuously as shown in Figs. 5(f) and 6(f), the coefficient reformulation presented in Section 4 does not suffer from these problems and the expected tracking performance is maintained. It should be noted that the responses in the case of $\pm 2g$ and $\pm 3g$ are similar, and the expected performance could be obtained for the $\pm 3g$ acceleration commands unlike the conventional control methods (e.g. gain scheduling). Based on these numerical simulation results, we can conclude that the proposed method is very effective, and thus, suitable to be applied to strongly coupled ship-to-ship missiles.

6. CONSLUSIONS

This paper presented a design method for the MIMO nonlinear autopilot, and also discussed the stability analysis for the ship-to-ship missiles with strong couplings between roll, yaw, and pitch axial dynamics. First, we proposed a control loop structure for roll, yaw, and pitch autopilot which can determine the required angles of all three control fins. For yaw and pitch autopilot design, missile model is reduced to a minimum phase model by applying a singular perturbation like technique and a MIMO nonlinear autopilot is designed. By considering the couplings between the roll, yaw, and pitch channel, a multi-input multi-output controller was proposed to realize a decoupled acceleration tracking performance. And the stability is analyzed considering roll influences on dynamic couplings of yaw and pitch channel as well as the aerodynamic couplings. Since we have designed the autopilot for an ideal missile model and did not consider any issues on its implementation and robustness, the performance and stability could be degraded by some kind of aerodynamic uncertainties or in a digital environment. Future works on this MIMO nonlinear autopilot design should focus on the practical design method considering the uncertainties and digital implementation.

NOMENCLATURE

$A_y(A_z)$:	Yaw (Pitch) achieved acceleration
$A_{yc}(A_{zc})$:	Yaw (Pitch) commanded acceleration
F_x, F_y, F_z:	X–, Y–, Z– components of the vector of aerodynamic forces
g_x, g_y, g_z:	X–, Y–, Z– components of the vector containing gravitational forces
$I \in R^{3\times3}$:	Moment of inertia of the airframe represented in the body axis
I_x, I_y, I_z:	X–, Y–, Z– components of the moment of inertia of the missile
I_{xy}, I_{yz}, I_{zx}:	Products of inertia
m, ρ:	Missile mass and air density
V_M:	Total velocity of missile $(= \sqrt{(U^2 + V^2 + W^2)})$

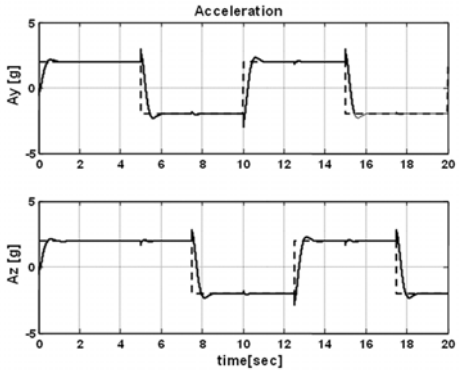

(a) Accelerations.

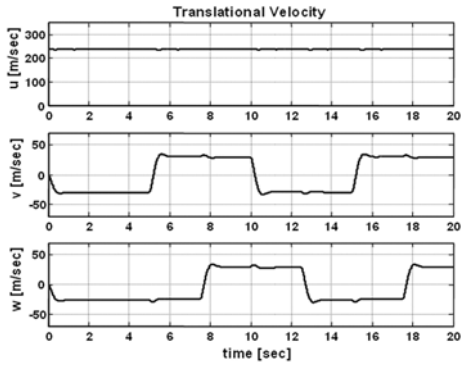

(b) Axial velocities.

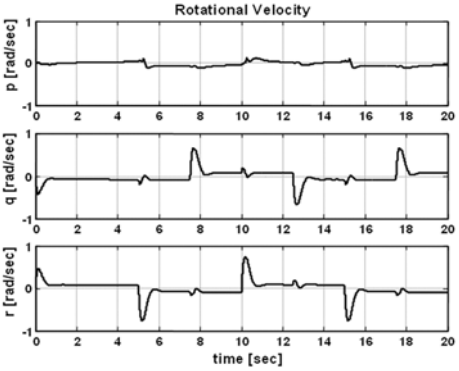

(c) Angular rates.

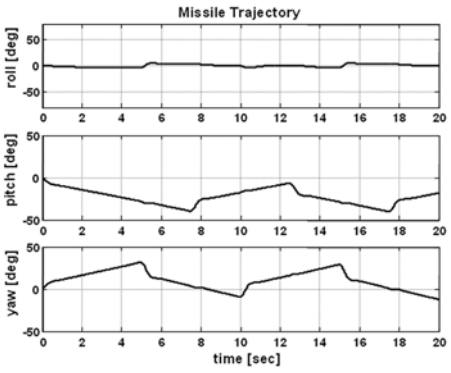

(d) Euler angles.

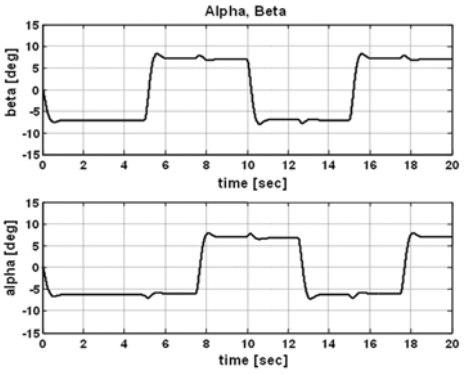

(e) Angle-of-attack and side slip angle.

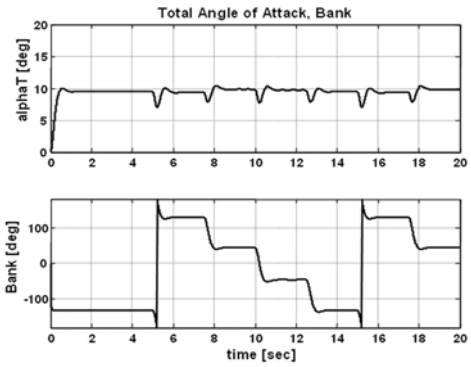

(f) Total angle-of-attack and bank angle.

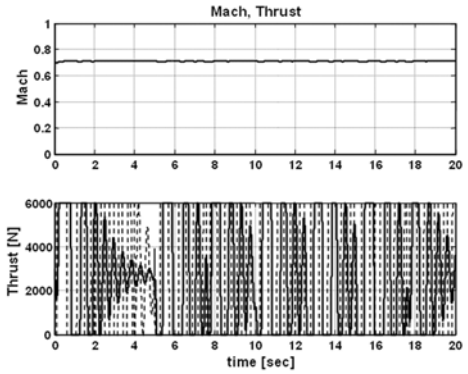

(g) Thrust.

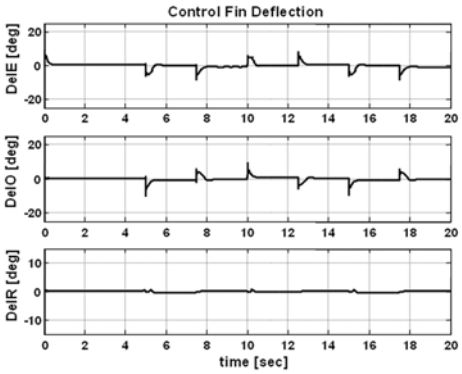

(h) Control fin deflections.

Fig. 5. Simulation results with acceleration command $A_{y(z)c} = \pm 2g$. (In (a), (g), and (h), solid: achieved, dotted: commanded).

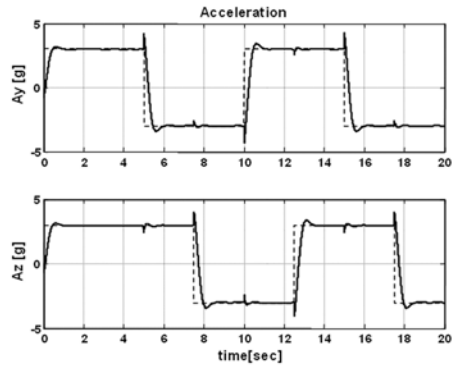

(a) Accelerations.

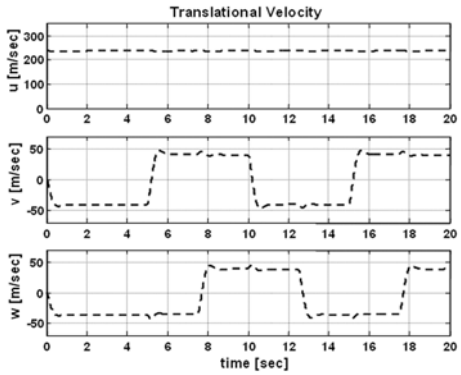

(b) Axial velocities.

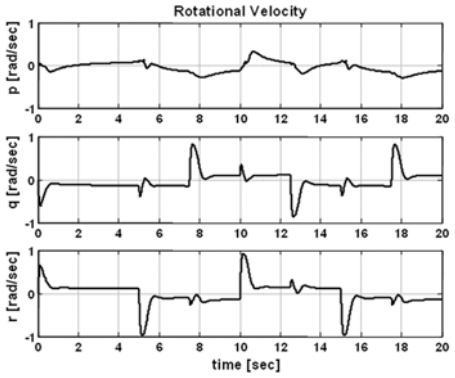

(c) Angular rates.

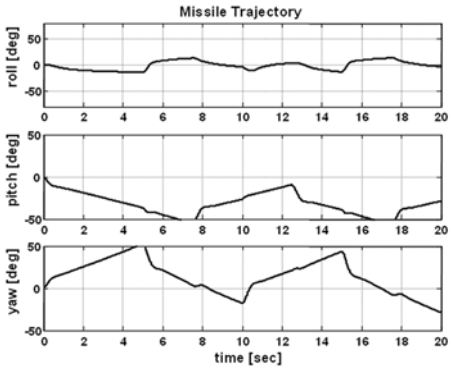

(d) Euler angles.

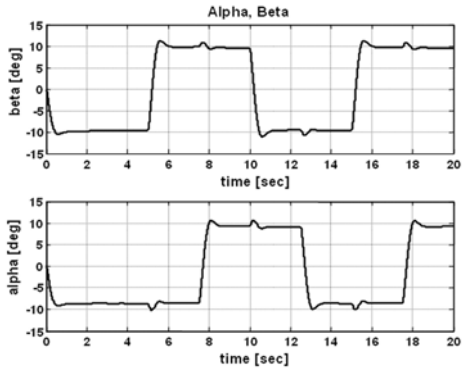

(e) Angle-of-attack and side slip angle.

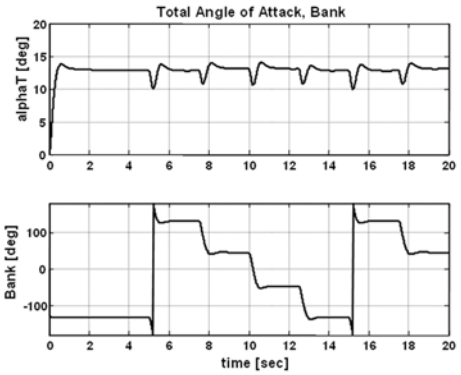

(f) Total angle-of-attack and bank angle.

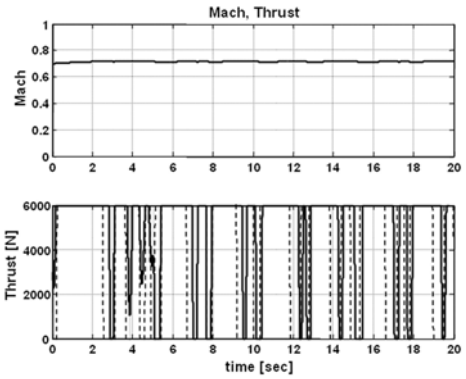

(g) Thrust.

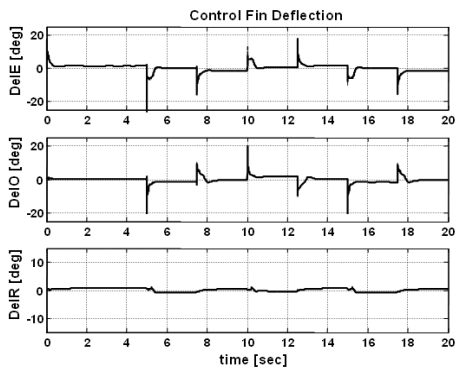

(h) Control fin deflections.

Fig. 6. Simulation results with acceleration command $A_{y(z)c} = \pm 3g$. (In (a), (g), and (h), solid: achieved, dotted: commanded.

M_M : Mach number $(=V_M/V_S)$

M_x, M_y, M_z: X–, Y–, Z– components of the vector of aerodynamic moments

p, q, r : X–, Y–, Z– components of the angular velocity vector of the missile

Q : Dynamic Pressure $(=\rho|V_M|^2/2)$

S , D : Aerodynamic reference area and length of the missile

T : Thrust force

U, V, W : X–, Y–, Z– components of the linear velocity vector of the missile

V_S : Velocity of sound

(X, Y, Z) : Missile body coordinate system

$\dot{x}$: Derivative of x with respect to time

$\|x\|$: Euclidean norm of the vector $x \in R^n$

$\|x\|_\infty$: $\sup_{t\geq 0}\|x(t)\|$

α, β : Angle-of-attack and sideslip angle in radians:
$(\alpha = \tan^{-1}(W/U),\ \ \beta = \tan^{-1}(V/U))$

α_T , ϕ_A : Total angle-of-attack and bank angle
$(\alpha_T = \tan^{-1}(\sqrt{V^2+W^2}/U),$
$\phi_A = \tan^{-1}(V/W))$

$\delta_E, \delta_O, \delta_R$: Deflection of Even, Odd, and Roll control fin; Even and odd control fins are approximately related with axial control fins as follows:
$\delta_E \cong \delta_q + \delta_r$, $\delta_O \cong -\delta_q + \delta_r$

$\delta_E^c, \delta_O^c, \delta_R^c$: Yaw, Pitch, and Roll fin command

APPENDIX A: PROOF OF THEOREM 1

The first and second rows in (24) can be augmented in matrix form as

$$\dot{w} = A_{11}w + A_{12}e_0, \tag{A1}$$

where

$$w = \begin{pmatrix} e_v \\ e_\eta \end{pmatrix}, \quad A_{11} = \begin{bmatrix} -\theta_1 & 0 & -\theta_2 & 0 \\ 0 & -\theta_1 & 0 & -\theta_2 \\ 1 & 0 & 0 & 0 \\ 0 & 1 & 0 & 0 \end{bmatrix},$$

$$A_{12} = \frac{-\theta_2 h_v}{m(Xh_v + D)} \times \begin{bmatrix} (HUC_{nr} - K_r I_M) & 0 \\ 0 & (HUC_{mq} + K_q I_M) \\ 0 & 0 \\ 0 & 0 \end{bmatrix}.$$

Here we derive the upper bound of norms $\|e_v(t)\|$, $\|e_\eta(t)\|$, $\|e_A(t)\|$, and $\|e_0(t)\|$ as follows:

Since A_{11} is a Hurwiz matrix for $\theta_1, \theta_2 > 0$, there exists a positive definite matrix P satisfying

$$A_{11}^T P + P A_{11} = -Q \tag{A2}$$

for some positive definite matrix Q. Define Lyapunov function candidates as

$$V_1 = \frac{1}{2} w^T P w, \quad V_2 = \frac{1}{2} e_0^T e_0. \tag{A3}$$

Differentiating V_1 with respect to time, and using (A1), (A2), and (A3), we have

$$\begin{aligned} \dot{V}_1 &= \frac{1}{2}(w^T A_{11}^T + e_0^T A_{12}^T) P w + \frac{1}{2} w^T P (A_{11} w + A_{12} e_0) \\ &= \frac{1}{2} w^T (A_{11}^T P + P A_{11}) w + \frac{1}{2}(e_0^T A_{12}^T P w + w^T P A_{12} e_0) \\ &\leq -\frac{1}{2} w^T Q w + \lambda_M(P) \cdot \|\theta_3\| \cdot \|w\| \cdot \|e_0\| \\ &\leq -\frac{\lambda_m(Q)}{\lambda_M(P)} V_1 + \lambda_M(P) \cdot \|\theta_3\| \cdot \|e_0\| \cdot \sqrt{2} \frac{\sqrt{V_1}}{\sqrt{\lambda_m(P)}}, \end{aligned}$$

where $\lambda_M(P)$ and $\lambda_m(P)$ are the maximum and minimum eigenvalues of matrix P, respectively and the vector θ_3 is defined as follows:

$$\theta_3 \equiv \begin{pmatrix} \dfrac{\theta_2 h_v (HUC_{nr} - K_r I_M)}{m(Xh_v + D)} \\ \dfrac{\theta_2 h_v (HUC_{nr} + K_q I_M)}{m(Xh_v + D)} \end{pmatrix}.$$

If we define $\upsilon_1 \equiv \sqrt{V_1}$, above inequality yields

$$\dot{\upsilon}_1 \leq -\frac{\lambda_m(Q)}{2\lambda_M(P)} \upsilon_1 + \frac{\lambda_M(P)}{\sqrt{2\lambda_m(P)}} \|\theta_3\| \cdot \|e_0\|. \tag{A4}$$

Integrating above equation with respect to time gives

$$\begin{aligned} \upsilon_1(t) \leq \upsilon_1(0) e^{-\sigma t} + \frac{\lambda_M(P)}{\sqrt{2\lambda_m(P)}} \\ \times \int_0^t \|\theta_3\| \cdot \|e_0(\tau)\| \cdot e^{-\sigma(t-\tau)} d\tau, \end{aligned} \tag{A5}$$

where $\sigma = \lambda_m(Q)/2\lambda_M(P) > 0$. Hence, from (A3) and (37), (A5) yields

$$\begin{aligned} \|e_v(t)\|, \|e_\eta(t)\| &\leq S_1^* e^{-\sigma t} \\ &\quad + S_2^* \int_0^t \|\theta_3\| \cdot \|e_0(\tau)\| \cdot e^{-\sigma(t-\tau)} d\tau, \end{aligned} \tag{A6a}$$

$$\begin{aligned} \|e_A(t)\| \leq \|e_\eta(t)\| + \|e_0(t)\| &\leq S_1^* e^{-\sigma t} \\ &\quad + S_2^* \int_0^t \|\theta_3\| \cdot \|e_0(\tau)\| \cdot e^{-\sigma(t-\tau)} d\tau + \|e_0(t)\|, \end{aligned} \tag{A6b}$$

where

$$S_1^* = \sqrt{\frac{2}{\lambda_m(P)}}\upsilon_1(0), \quad S_2^* = \frac{\lambda_M(P)}{\lambda_m(P)}.$$

Now, we take the time derivative of V_2 in (A3) and proceed as in V_1 to obtain

$$\|e_0(t)\| \le \|e_0(0)\|e^{-\|A_2\|t} + \int_0^t \|\dot{h}(\tau)\| \cdot e^{-\|A_2\|(t-\tau)} d\tau \quad \text{(A7)}$$

From (A6a), (A6b), and (A7), the boundedness of e_v, e_η, e_{Ay}, e_0 depends on that of $\dot{h}$.

We take $\dot{h}(\alpha, \beta, u_y, u_z)$ into account. By using (22), the time derivative of (28) becomes

$$\begin{aligned}\frac{d}{dt}h(\alpha,\beta,u_y,u_z) &= \frac{d}{dt}\begin{pmatrix} h_y \\ h_z \end{pmatrix} \\ &= \left\{ -\frac{(BX_{cg}-1)(X_{cg}h_v + D)m}{I_M(h_v + DB)} \cdot A_2^{-1} \right. \\ &\quad \left. + p\frac{UQSD}{I_M(h_v + DB)} \cdot A_2^{-1} \cdot A_{uv}^{-1} \right\} \cdot \begin{pmatrix} v_y \\ v_z \end{pmatrix} \\ &\quad - \frac{Um(X_{cg}h_v + D)}{I_M(h_v + DB)} \cdot A_2^{-1} \cdot \left\{ \begin{pmatrix} \frac{\dot{u}_y}{U} \\ -\frac{\dot{u}_z}{U} \end{pmatrix} - \begin{pmatrix} \dot{p}\beta \\ \dot{p}\alpha \end{pmatrix} \right\},\end{aligned} \quad \text{(A8)}$$

and again, taking the time derivative of (14), we have

$$\begin{aligned}\frac{1}{U}\dot{u} &= \left(\frac{QSD}{(X_{cg}h_v + D)m} \right)^{-1} \cdot \left\{ \frac{d}{dt}(A_{uv}^{-1}) - \theta_1 \cdot A_{uv}^{-1} \right\} \cdot v \\ &\quad + \left(\frac{QSD}{(X_{cg}h_v + D)m} \right)^{-1} \cdot \theta_2 \cdot A_{uv}^{-1} \cdot e_{YZ}\end{aligned} \quad \text{(A9)}$$

and

$$\begin{aligned}\frac{1}{U}\|\dot{u}\| &\le \left(\frac{QSD}{(X_{cg}h_v + D)m} \right)^{-1} \cdot \|A_{uv}^{-1}\| \\ &\quad \times \left(\theta_{uv} \cdot \|v\| + \theta_2 \cdot \|e_{YZ}\| \right) \\ &= u_1^* \cdot \|v\| + u_2^* \cdot \|e_{YZ}\|,\end{aligned} \quad \text{(A10)}$$

where θ_{uv} is a positive constant which satisfies

$$\left\| \frac{d}{dt}(A_{uv}^{-1}) - \theta_1 \cdot A_{uv}^{-1} \right\| \le \theta_{uv} \cdot \|A_{uv}^{-1}\| \quad \text{(A11)}$$

and u_1^* and u_2^* are given as

$$u_1^* = \theta_{uv}\|A_{uv}^{-1}\|, \quad u_2^* = \theta_2\|A_{uv}^{-1}\|. \quad \text{(A12)}$$

The derivation of (A11) is given in Appendix B.

From the fourth condition of Assumption 3, u_1^* and u_2^* are bounded independent of α and β. Also, from Proposition 1, the stabilized dynamics of reduced system result in

$$|v(t)| \le \lambda_v, \quad \left\| \begin{pmatrix} A_{yc}(t) - \bar{A}_y(t) \\ A_{zc}(t) - \bar{A}_z(t) \end{pmatrix} \right\| \le \lambda_A \quad \text{(A13)}$$

for some positive constants λ_v and λ_A. As can be seen in (13), it should be noted that λ_A is a bound converging to zero asymptotically. Thus, we have inequalities

$$\|v\|_\infty \le \lambda_v + \|e_v\|_\infty, \quad \|e_{YZ}\|_\infty \le \lambda_A + \|e_A\|_\infty \quad \text{(A14)}$$

and (A10) yields

$$\begin{aligned}\frac{1}{U}\|\dot{u}\|_\infty &\le u_1^*(\lambda_v + \|e_v\|_\infty) + u_2^*(\lambda_A + \|e_A\|_\infty) \\ &= u_1^* \cdot \|e_v\|_\infty + u_2^* \cdot \|e_A\|_\infty + (u_1^* \cdot \lambda_v + u_2^* \cdot \lambda_A).\end{aligned} \quad \text{(A15)}$$

Combining (A8), (A14), and (A15), we have the inequality

$$\begin{aligned}\left\| \frac{d}{dt}h(\alpha,\beta,u_y,u_z) \right\| &\le \eta_1^* \cdot \|v\|_\infty + \eta_2^* \cdot \left\| \frac{\dot{u}}{U} \right\|_\infty + \eta_3^* \\ &\le (\eta_1^* + u_1^*\eta_2^*)\|e_v\|_\infty + u_2^*\eta_2^*\|e_A\|_\infty + \lambda_v\eta_1^* \\ &\quad + (u_1^*\lambda_v + u_2^*\lambda_A)\eta_2^* + \eta_3^* \\ &= h_1^*\|e_v\|_\infty + h_2^*\|e_A\|_\infty + h_3^*,\end{aligned} \quad \text{(A16)}$$

where

$$\begin{aligned}\eta_1^* &= \|A_2^{-1}\| \cdot \left\| -\frac{(BX_{cg}-1)(X_{cg}h_v + D)m}{I_M(h_v + DB)} \right. \\ &\quad \left. + p\frac{UQSD}{I_M(h_v + DB)} \cdot A_{uv}^{-1} \right\|, \\ \eta_2^* &= \frac{Um(X_{cg}h_v + D)}{I_M(h_v + DB)} \cdot \|A_2^{-1}\|, \\ \eta_3^* &= \frac{Um(X_{cg}h_v + D)}{I_M(h_v + DB)} \cdot \|A_2^{-1}\| \cdot \left\| \begin{pmatrix} \dot{p}\beta \\ \dot{p}\alpha \end{pmatrix} \right\|, \\ h_1^* &= \eta_1^* + u_1^*\eta_2^*, \\ h_2^* &= u_2^*\eta_2^*, \\ h_3^* &= \lambda_v\eta_1^* + (u_1^*\lambda_v + u_2^*\lambda_A)\eta_2^* + \eta_3^*.\end{aligned}$$

After several algebraic operations, we have the inequality

$$\begin{aligned}&\int_0^t \left\| \frac{d}{dt}h(\alpha,\beta,u_y,u_z) \right\| e^{-\|A_2\|(t-\tau)} d\tau \\ &\le H_1^* e^{-\sigma t} + H_2^* + \int_0^t H_3^* \|e_0(\tau)\| \cdot e^{-\sigma(t-\tau)} d\tau,\end{aligned} \quad \text{(A17)}$$

where

$$H_1^* = \frac{h_1^* + h_2^*}{\|A_2\| - \sigma} S_1^*, \quad H_2^* = \frac{h_3^*}{\|A_2\|},$$
$$H_3^* = \frac{h_1^* + h_2^*}{\|A_2\| - \sigma} S_2^* \|\theta_3\| + h_2^*.$$

For the proof of (A17), see Appendix C.

Substituting (A17) into (A7) and using Gronwall-Bellman Inequality [13], we have

$$\begin{aligned} \|e_0(t)\| \;\le\; & \|e_0(0)\| e^{-\|A_2\|t} + H_1^* e^{-\sigma t} + H_2^* \\ & + \int_0^t \left(\|e_0(0)\| e^{-\|A_2\|t} + H_1^* e^{-\sigma t} + H_2^* \right) H_3^* \\ & \times e^{-\sigma(t-\tau)} \cdot \exp\left(\int_\tau^t H_3^* e^{-\sigma(t-\zeta)} d\zeta \right) d\tau \end{aligned} \quad \text{(A18)}$$

and this yields

$$\begin{aligned} \|e_0(t)\| \;\le\; & \|e_0(0)\| e^{-\|A_2\|t} + H_1^* e^{-\sigma t} + H_2^* \\ & + H_3^* \cdot e^{\frac{H_3^*}{\sigma}} \left(\frac{\|e_0(0)\|}{\|A_2\| - \sigma} (e^{-\sigma t} - e^{-\|A_2\|t}) \right. \\ & \left. + \frac{H_1^* + eH_2^*}{\sigma e} \right), \end{aligned} \quad \text{(A19)}$$

where e is the base of natural logarithm. In (A18), H_i^*, $i = 1,2,3$, are all bounded and the other terms are exponentially decaying. Therefore, from Assumption 2, the steady state error of $e_0(t)$ will be bounded as

$$\|e_0(t)\|_{ss} \;\le\; H_2^* + H_3^* \cdot e^{\frac{H_3^*}{\sigma}} \left(\frac{H_1^* + eH_2^*}{\sigma e} \right), \quad \text{(A20)}$$

and this bound depends on the initial values and design parameters. □

APPENDIX B: DERIVATION OF (A11)

The relation between $d(A_{uv}^{-1})/dt$ and A_{uv}^{-1} is shown by approximating the aerodynamic coefficients as polynomials. As in many researches [10,12], [15], the nonlinear aerodynamic coefficients can be fitted as polynomial functions with sufficient accuracy. Here, we define a function which describes the order of the given polynomial.

$$\text{order}[A] \equiv \text{the order of polynomial } A.$$

For simplicity, instead of using the original $C_a(\alpha, \beta)$, we assume that C_a is dependent on only β as in SISO system, and the Jacobian matrix in (9) is replaced with a scalar function defined as $A_{uv}(\beta) \equiv \partial C_a / \partial \beta$; Since we can proceed with $C_a(\alpha, \beta)$ in the same manner. Suppose that original coefficient C_a can be approximated by an *n-th* order polynomial function in β with sufficient accuracy as

$$C_a(\beta) = \beta^n + a_{n-1}\beta^{n-1} + \cdots + a_0, \quad \text{(B1)}$$

$$\begin{aligned} A_{uv}(\beta) &= \frac{\partial C_a}{\partial \beta} \\ &= n\beta^{n-1} + a_{n-1}(n-1)\beta^{n-2} + \cdots + a_1. \end{aligned} \quad \text{(B2)}$$

From (32a), we have

$$\begin{aligned} \frac{d}{dt}(A_{uv}^{-1}) &= -\frac{\partial A_{uv}}{\partial \beta} \cdot \frac{1}{(A_{uv})^2} \dot{\beta} \\ &= -\frac{\partial A_{uv}}{\partial \beta} \cdot \frac{1}{(A_{uv})^2} v_y \cdot \frac{1}{A_{uv}} = A^* \cdot A_{uv}^{-1}. \end{aligned} \quad \text{(B3)}$$

where

$$\begin{aligned} A^* &= -\frac{\partial A_{uv}}{\partial \beta} \cdot \frac{1}{(A_{uv})^2} v_y \\ &= -\frac{n(n-1)\beta^{n-2} + \cdots + a_2}{(n\beta^{n-1} + a_{n-1}(n-1)\beta^{n-2} + \cdots + a_1)^2} v_y. \end{aligned} \quad \text{(B4)}$$

From (23), we have

$$\text{order}[v_y] \;\le\; \text{order}[A_y] = \text{order}[C_a] = n.$$

Also, checking the order of v_y in (B4), the order of A^* is lower than or equal to zero, i.e.,

$$\text{order}[A^*] \le 0.$$

Accordingly, from the second condition of Assumption 3 and (B2), the denominator polynomial of A^* is positive and also independent of the value of β; thus, A^* can be bounded for some proper constant λ_β as

$$\|A^*\| \le \lambda_\beta,$$

which yields

$$\left\| \frac{d}{dt}(A_{uv}^{-1}) \right\| \le \lambda_\beta \|A_{uv}^{-1}\|.$$

Finally, (A11) can be described again as

$$\left\| \frac{d}{dt}(A_{uv}^{-1}) - \theta_1 \cdot A_{uv}^{-1} \right\| \;\le\; (\lambda_\beta + 1)\|A_{uv}^{-1}\| \;=\; \theta_{uv}\|A_{uv}^{-1}\|,$$

where $\theta_{uv} = \lambda_\beta + 1$.

APPENDIX C: PROOF OF (A17)

$$\int_0^t \left\| \frac{d}{dt} h(\alpha, \beta, u_y, u_z) \right\| e^{-\|A_2\|(t-\tau)} d\tau$$

$$\le \int_0^t \left(h_1^* \|e_v(\tau)\| + h_2^* \|e_A(\tau)\| + h_3^* \right) e^{-\|A_2\|(t-\tau)} d\tau$$

$$\le \int_0^t \left(h_1^* \|e_v(\tau)\| + h_2^* \|A_1\| \cdot \|e_0(\tau)\| + h_2^* \|e_\eta(\tau)\| + h_3^* \right) \times e^{-\|A_2\|(t-\tau)} d\tau$$

$$\le (h_1^* + h_2^*) \left\{ S_1^* \frac{1}{\|A_2\| - \sigma} (e^{-\sigma t} - e^{-\|A_2\| t}) + S_2^* \|\theta_3\| \cdot \|e_0(t)\| * e^{-\sigma t} * e^{-\|A_2\| t} \right\} + \int_0^t h_2^* \|A_1\| \cdot \|e_0(\tau)\| \cdot e^{-\|A_2\|(t-\tau)} d\tau + \frac{h_3^*}{\|A_2\|} (1 - e^{-\|A_2\| t})$$

$$\le \left\langle \frac{h_1^* + h_2^*}{\|A_2\| - \sigma} S_1^* e^{-\sigma t} \right\rangle + \left\langle \frac{h_3^*}{\|A_2\|} \right\rangle + \left\langle \frac{h_1^* + h_2^*}{\|A_2\| - \sigma} S_2^* \|\theta_3\| \cdot \|e_0(t)\| * (e^{-\sigma t} - e^{-\|A_2\| t}) + \int_0^t h_2^* \|A_1\| \cdot \|e_0(\tau)\| \cdot e^{-\sigma(t-\tau)} d\tau \right\rangle$$

$$\le \left\langle H_1^* e^{-\sigma t} \right\rangle + \left\langle H_2^* \right\rangle + \left\langle \int_0^t H_3^* \|e_0(\tau)\| \cdot e^{-\sigma(t-\tau)} d\tau \right\rangle,$$

where

$$H_1^* = \frac{h_1^* + h_2^*}{\|A_2\| - \sigma} S_1^*, \quad H_2^* = \frac{h_3^*}{\|A_2\|},$$

$$H_3^* = \frac{h_1^* + h_2^*}{\|A_2\| - \sigma} S_2^* \|\theta_3\| + h_2^*.$$

Substituting (A16) into (A7), we have the first inequality. The second and third inequalities come from (16) and (A6a), respectively. In the fourth inequality, we used the condition, $0 < \sigma < \|A_2\|$. □

REFERENCES

[1] M. Tahk, M. Briggs, and P. K. A. Menon, "Applications of plant inversion via state feedback to missile autopilot design," *Proc. of the Conference on Decision and Control*, pp. 730-735, 1988.

[2] K.-Y. Lian, L.-C. Fu, D.-M. Chuang, and T.-S. Kuo, "Nonlinear autopilot and guidance for a highly maneuverable missile," *Proc. of the American Control Conference*, pp. 2293-2297, 1994.

[3] R. A. Hull, D. Schumacher, and Z. Qu, "Design and evaluation of robust nonlinear missile autopilots from a performance perspective," *Proc. of the American Control Conference*, pp. 189-193, 1995.

[4] R. A. Hull and Z. Qu, "Dynamic robust recursive control design and its application to a nonlinear missile autopilot," *Proc. of the American Control Conference*, pp. 833-837, 1997.

[5] J. Huang and C.F. Lin, "Sliding mode control of HAVE DASH II missile systems," *Proc. of American Control Conference*, pp. 183-187, 1993.

[6] J. Huang, C. F. Lin, J. R. Cloutier, J. H. Evers, and C. D'Souza, "Robust feedback linearization approach to autopilot design," *Proc. of the IEEE Conference on Control Applications*, pp. 220-225, 1992.

[7] J. J. Romano and S. N. Singh, "I-O map inversion, zero dynamics and flight control," *IEEE Trans. on Aerospace and Electronic Systems*, vol. 26, no. 6, pp. 1022-1028, December 1990.

[8] S. N. Singh and M. Steinberg, "Adaptive control of feedback linearizable nonlinear systems with application to flight control," *Journal of Guidance, Control, and Dynamics*, vol. 19, no. 4, pp. 871-877, August 1996.

[9] V. H. L. Cheng, C. E. Njaka, and P. K. Menon, "Practical design methodologies for robust nonlinear flight control," *Proc. of AIAA, Guidance Navigation and Control Conference*, 96-3785, 1996.

[10] J. I. Lee, J. H. Oh, I. J. Ha, E. G. Kim, and H. J. Cho, "A new approach to autopilot design for highly nonlinear missiles," *Proc. of AIAA, Guidance Navigation and Control Conference*, 96-3915, 1996.

[11] J. H. Oh and I. J. Ha, "Missile autopilot design via functional inversion and time-scaled transformation," *IEEE Trans. on Aerospace and Electronic Systems*, vol. 33, no. 1, pp. 64-76, January 1997.

[12] D. Chwa and J. Y. Choi, "New parametric affine modeling and control for skid-to-turn missiles," *IEEE Trans. on Control Systems Technology*, vol. 9, no. 2, pp. 335-347, March 2001.

[13] H. K. Khalil, "Exact feedback linearization," *Nonlinear Systems*, 2nd edition, Prentice Hall, New Jersey, 1996.

[14] A. Isidori, "Elementary theory of nonlinear feedback for multi-input multi-output systems," *Nonlinear Control System*, 3rd ed., Springer-Verlag, London, 1995.

[15] J. H. Blakelock, *Automatic Control of Aircraft and Missiles*, 2nd ed., John Wiley & Sons Inc., New York, 1991.

Ki Hong Im received the B.S., M.S. degree in Mechanical Engineering from Pusan National University in 1999, 2001, respectively, and the Ph.D. degree in Electrical Eng. and Computer Science from Seoul National University in 2006. His research interests include nonlinear systems and adaptive control.

Dongkyoung Chwa received the B.S., M.S., and Ph.D. degree in Electrical Engineering and Computer Science from Seoul National University in 1995, 1997, 2001, respectively. His research interests include nonlinear systems, and adaptive and robust control.

Jin Young Choi received the B.S., M.S., and Ph.D. degree in Electrical Engineering and Computer Science from Seoul National University in 1982, 1984, 1993, respectively. His research interests include intelligent systems and adaptive control.